Microscopic analysis of the octupole phase transition in Th isotopes

Nomura, Kosuke; Vretenar, Dario; Lu, Bing-nan

PHYSICAL REVIEW C **88**, 021303(R) (2013)

Microscopic analysis of the octupole phase transition in Th isotopes

K. Nomura,[1,2] D. Vretenar,[2] and B.-N. Lu[3,2]
[1]*Institut für Kernphysik, Universität zu Köln, D-50937 Köln, Germany*
[2]*Physics Department, Faculty of Science, University of Zagreb, 10000 Zagreb, Croatia*
[3]*State Key Laboratory of Theoretical Physics, Institute of Theoretical Physics, Chinese Academy of Sciences, Beijing 100190, China*
(Received 27 March 2013; revised manuscript received 19 July 2013; published 19 August 2013)

A shape phase transition between stable octupole deformation and octupole vibrations in Th nuclei is analyzed in a microscopic framework based on nuclear density functional theory. The relativistic density dependent point coupling (DD-PC1) functional is used to calculate axially symmetric quadrupole-octupole constrained energy surfaces. Observables related to order parameters are computed using an interacting-boson Hamiltonian, with parameters determined by mapping the microscopic energy surfaces to the expectation value of the Hamiltonian in the boson condensate. The systematics of constrained energy surfaces and low-energy excitation spectra point to the occurrence of a phase transition between octupole-deformed shapes and shapes characterized by octupole-soft potentials.

DOI: 10.1103/PhysRevC.88.021303 PACS number(s): 21.10.Re, 21.60.Ev, 21.60.Fw, 21.60.Jz

The evolution of equilibrium shapes and the corresponding excitation dynamics present one of the most intriguing aspects of the nuclear many-body system [1–3]. The simplest low-energy collective excitations correspond to quadrupole modes, that is, the geometrical shape of a nucleus varies between a sphere and a rotational ellipsoid. Most deformed nuclei display quadrupole reflection-symmetric equilibrium shapes, and the corresponding excitation spectra are characterized by positive-parity rotational bands. There are, however, regions of the mass table in which octupole deformations (reflection-asymmetric, pearlike shapes) occur [4]. Reflection-asymmetric shapes are distinguished by the presence of negative-parity bands, and by pronounced electric dipole and octupole transitions. Structure phenomena related to reflection-asymmetric nuclear shapes have been explored in numerous studies [4–19]. Analogous excitation patterns are also observed in other mesoscopic systems such as molecules and, therefore, studies of octupole collective degrees of freedom are of broad interest in many aspects of finite quantum systems.

The transition between different nuclear shapes in most isotopic or isotonic sequences is gradual. In some cases, however, the addition/subtraction of only a few nucleons leads to rather rapid changes in equilibrium shapes and, in particular, shape phase transitions and critical-point phenomena may occur. Phase transitions in the equilibrium shapes of nuclei correspond to first- and second-order quantum phase transitions (QPTs) between competing ground-state phases induced by variation of a nonthermal control parameter (number of nucleons) at zero temperature [20]. Important issues in studies of nuclear QPT include the identification of observables that can be related to order parameters, the degree to which discontinuities at a phase transitional point are smoothed out in finite nuclei, and the question of how precisely can a point of phase transition be associated with a particular isotope, considering that the control parameter, i.e., nucleon number, is not continuous but takes only discrete integer values. In the last decade nuclear QPTs have been investigated extensively, both in experimental studies and employing a variety of theoretical models (cf. Ref. [20] for a recent review). Most studies have been focused on quadrupole shape phase transitions, but several phenomenological models have also considered possible phase transitions related to octupole shapes [5,10,12–17].

In this Rapid Communication we analyze shape QPTs in octupole deformed nuclei and present the first microscopic realization of a QPT from stable octupole deformation to octupole vibrations in the Th isotopic chain, characteristic for the region of light actinides. This study is based on the microscopic framework of nuclear energy density functionals, and a corresponding interacting boson model [21] Hamiltonian is constructed to calculate the excitation spectra and observables that can be related to quantum order parameters.

At present the most comprehensive approach to nuclear structure is based on the framework of energy density functionals (EDFs). Nuclear EDFs enable a complete and accurate description of ground-state properties and collective excitations over the whole nuclide chart [22]. Both nonrelativistic and relativistic EDFs have successfully been applied to the description of the evolution of single-nucleon shell structures and the related shape-transition and shape-coexistence phenomena. The calculations reported in this Rapid Communication are based on the relativistic EDF density dependent point coupling (DD-PC1) [23]. This functional has been employed in a number of mean-field and beyond-mean-field studies of structure phenomena in various mass regions [24], from the evolution of shapes in $N = 28$ isotones [25], to rapid shape transitions in superheavy nuclei [26]. Rather than using a specifically designed potential model that by construction describes the critical point of octupole phase transition [12–16], here we employ a global density functional that was not specifically adjusted nor ever before applied to studies of octupole shapes and negative-parity states.

The analysis starts by performing constrained self-consistent relativistic mean-field calculations for axially symmetric shapes in the (β_2,β_3) plane, with constraints on the mass quadrupole Q_{20}, and octupole Q_{30} moments. The dimensionless shape variables β_λ $(\lambda = 2, 3)$ are defined in terms of the multipole moments $Q_{\lambda 0}$: $\beta_\lambda \equiv (4\pi/3AR^\lambda)Q_{\lambda 0}$,

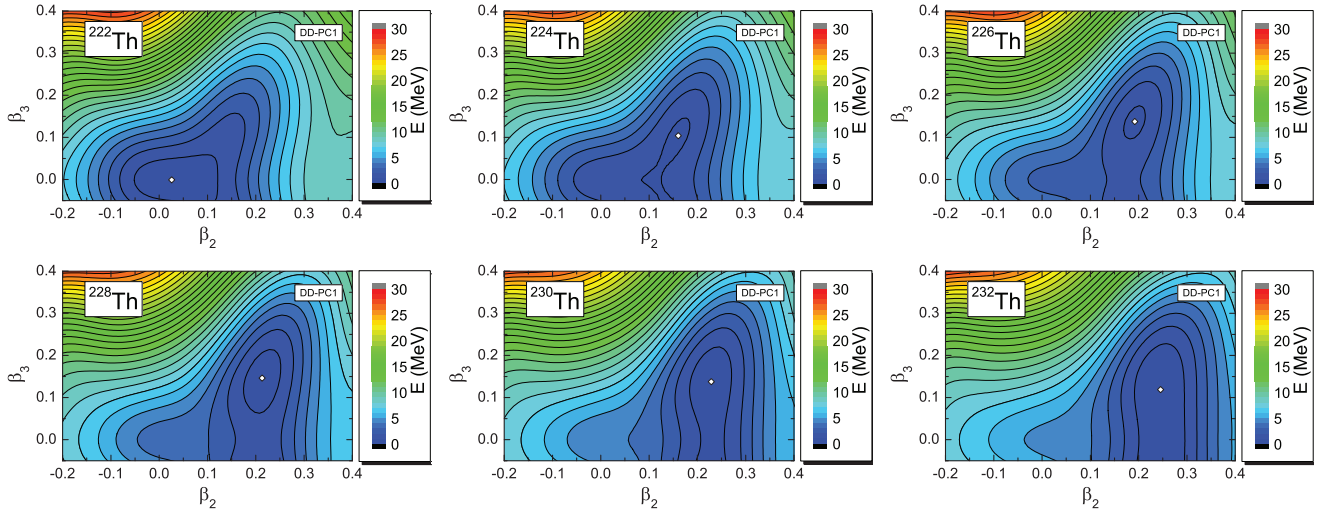

FIG. 1. (Color online) Microscopic DD-PC1 self-consistent relativistic Hartree-Bogoliubov (RHB) axially symmetric energy surfaces of the nuclei $^{222-232}$Th in the (β_2, β_3) plane, symmetric with respect to $\beta_3 = 0$ axis. The contours join points on the surface with the same energy, and the separation between neighboring contours is 1 MeV. In each panel, the minimum is indicated by a open diamond.

with $R = 1.2A^{1/3}$ fm. The relativistic Hartree-Bogoliubov (RHB) model [27] is used to calculate constrained energy surfaces (cf. [28] for details), the functional in the particle-hole channel is DD-PC1, and pairing correlations are taken into account by employing an interaction that is separable in momentum space and is completely determined by two parameters adjusted to reproduce the empirical bell-shaped pairing gap in symmetric nuclear matter [24,29].

Figure 1 displays the contour plots of deformation energy surfaces in the (β_2,β_3) plane for the isotopes $^{222-232}$Th. The plots are symmetric with respect to the $\beta_3 = 0$ axis. Already at the mean-field level the RHB model predicts a very interesting structural evolution. A soft energy surface is calculated for ^{222}Th, with the energy minimum close to $(\beta_2, \beta_3) \approx (0, 0)$. The quadrupole deformation becomes more pronounced in ^{224}Th, and one also notices the development of octupole deformation. The energy minimum is found in the $\beta_3 \neq 0$ region, located at $(\beta_2, \beta_3) \approx (0.15, 0.1)$. From ^{224}Th to ^{226,228}Th a rather strongly marked octupole minimum is predicted. The deepest octupole minimum is calculated in ^{226}Th whereas, starting from ^{228}Th, the minimum becomes softer in β_3 direction. Soft octupole surfaces are obtained for ^{230,232}Th, the latter being completely flat in β_3.

A quantitative study of shape transitions must go beyond a simple mean-field calculation of potential energy surfaces and, particularly in the case of a possible QPT, it must include the computation of observables that can be related to quantum order parameters. In this Rapid Communication we employ the interacting boson model (IBM) [21] to calculate spectroscopic properties associated to quadrupole and octupole deformations. The building blocks of the IBM include the monopole s and the quadrupole d bosons, corresponding to collective $J^\pi = 0^+$ and 2^+ pairs of valence nucleons, respectively [30]. To describe reflection-asymmetric deformations and the corresponding negative-parity states, in addition to the positive-parity bosons, the model space must include the octupole $(J^\pi = 3^-)$ boson f [8,21]. Here we employ the following sdf-IBM Hamiltonian similar to the one used in Ref. [31]

$$\hat{H} = \epsilon_d \hat{n}_d + \epsilon_f \hat{n}_f + \kappa_2 \hat{Q} \cdot \hat{Q} + \alpha \hat{L}_d \cdot \hat{L}_d + \kappa_3 : \hat{V}_3^\dagger \cdot \hat{V}_3 : \quad (1)$$

where $\hat{n}_d = d^\dagger \cdot \tilde{d}$ and $\hat{n}_f = f^\dagger \cdot \tilde{f}$ denote the d and f boson number operators, respectively. The third term is the quadrupole-quadrupole interaction with the quadrupole operator $\hat{Q} = s^\dagger \tilde{d} + d^\dagger s + \chi_d [d^\dagger \times \tilde{d}]^{(2)} + \chi_f [f^\dagger \times \tilde{f}]^{(2)}$. The angular momentum operator in the sd space reads $\hat{L}_d = \sqrt{10}[d^\dagger \times \tilde{d}]^{(1)}$, and the last term in Eq. (1) denotes a specific octupole-octupole interaction expressed in normal-ordered form with $\hat{V}_3^\dagger = s^\dagger \tilde{f} + \chi_3 [d^\dagger \times \tilde{f}]^{(3)}$.

For each nucleus the Hamiltonian parameters: ϵ_d, ϵ_f, α, κ_2, κ_3, χ_d, χ_f, and χ_3, are determined by employing the procedure of Ref. [32]: the microscopic self-consistent mean-field energy surface is mapped onto the equivalent IBM energy surface, that is, on the expectation value of the IBM Hamiltonian $\langle\phi|\hat{H}|\phi\rangle$ in the boson condensate state $|\phi\rangle$ [33] (see Refs. [32,34] for details). $|\phi\rangle = \frac{1}{\sqrt{N_B!}}(\lambda^\dagger)^{N_B}|-\rangle$, with $\lambda^\dagger = s^\dagger + \beta_2 d_0^\dagger + \beta_3 f_0^\dagger$. N_B and $|-\rangle$ denote the number of bosons, that is, half the number of valence nucleons [30], and the boson vacuum (a core with doubly closed shells), respectively. In the present case the doubly magic nucleus ^{208}Pb plays the role of the boson vacuum. Thus, N_B varies between 6 and 12 for the $^{220-232}$Th nuclei. By equating the expectation value of the sdf IBM Hamiltonian as a function of β_2 and β_3 to the microscopic energy surface in the neighborhood of the minimum, the Hamiltonian parameters can be determined without invoking any further adjustment to data. Once the parameters are specified, the Hamiltonian of Eq. (1) is numerically diagonalized by using the code OCTUPOLE [35] to generate energy spectra and transition rates.

In Fig. 2 we plot the microscopically determined values of the IBM Hamiltonian parameters ϵ_d, ϵ_f, χ_d, χ_f, and χ_3 for Th isotopes, as functions of the mass number. The decrease of

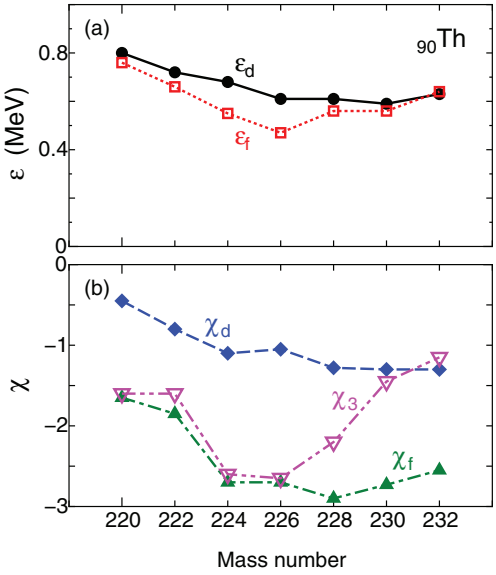

FIG. 2. (Color online) Variation of the derived parameters ϵ_d, ϵ_f, χ_d, χ_f, and χ_3 as functions of the mass number.

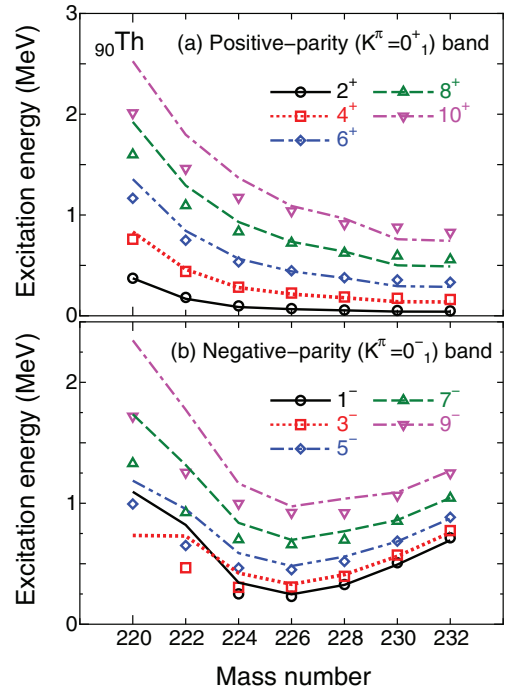

FIG. 3. (Color online) Isotopic dependence of the excitation energies of levels of the positive-parity ground-state band ($K^\pi = 0^+_1$) (a), and the lowest negative-parity band ($K^\pi = 0^-_1$) (b), for $^{220-232}$Th. In each panel lines and symbols denote the theoretical and the experimental [37] values, respectively.

the d-boson energy ϵ_d in Fig. 2(a) reflects the enhancement of quadrupole collectivity in heavier Th isotopes (cf. Fig. 1). ϵ_d is nearly constant from ^{226}Th up to ^{230}Th. The f-boson energy ϵ_f also decreases from ^{220}Th to ^{226}Th, and from that isotope its value increases with mass. An interesting feature to be noted in Fig. 2(a) is that ϵ_f is of the same order of magnitude as ϵ_d, and this implies that the octupole deformation can be as pronounced as the quadrupole one. In fact, the octupole minimum on the RHB energy surfaces is rather deep for $A \geqslant 226$ (Fig. 1). We note that, in contrast, most phenomenological sdf-IBM studies have assumed a rather weak coupling between positive and negative-parity bosons, $\epsilon_d \ll \epsilon_f$ [8].

Figure 2(b) shows that the quadrupole parameter χ_d increases in magnitude with A, and its value is close to the SU(3) limit of the sd IBM $\chi_d = -\sqrt{7}/2 \approx 1.3$ [21] for $A \geqslant 228$. In the same panel, both χ_f and χ_3 exhibit a rapid change from ^{222}Th to ^{224}Th, corresponding to the onset of quadrupole and octupole deformations. Starting from ^{226}Th, χ_f is rather constant, whereas the value of χ_3 decreases in magnitude reflecting the softness of the octupole minimum (Fig. 1).

Nearly constant values are adopted for the remaining strength parameters: $\kappa_2 \approx -0.06$ MeV and $\kappa_3 \approx -0.015$ MeV. The coupling constant of the $\hat{L}_d \cdot \hat{L}_d$ term $\alpha \approx -0.02$ MeV is determined separately so that the cranking moment of inertia in the IBM intrinsic state, corresponding to the minimum on the β_2 axis, becomes identical to the one computed in the mean-field model [36].

A signature of stable octupole deformation is a low-lying negative-parity band $J^\pi = 1^-, 3^-, 5^-, \ldots$ located close in energy to the positive-parity ground-state band $J^\pi = 0^+, 2^+, 4^+, \ldots$, thus forming an alternating-parity band. Such alternating bands are typically observed for states with spin $J \geqslant 5$ [4]. In the case of octupole vibrations the negative-parity band is found at higher energy, and the two sequences of positive- and negative-parity states form separate collective bands. Therefore, a systematic increase with nucleon number of the energy of the negative-parity band relative to the positive-parity ground-state band indicates a transition from stable octupole deformation to octupole vibrations [4].

In Fig. 3 we display the systematics of calculated excitation energies of the ground-state band ($K^\pi = 0^+_1$) and the lowest negative-parity band ($K^\pi = 0^-_1$) in $^{220-232}$Th, in comparison to available data [37]. For all isotopes these two bands are formed by zero f-boson and one f-boson states, respectively. Even without any adjustment to the data, that is, by simply using parameters determined by the microscopic calculation of potential energy surfaces, the IBM quantitatively reproduces the isotopic dependence of excitation energies of levels belonging to the lowest bands of positive and negative parity.

Positive-parity levels, shown in Fig. 3(a), systematically decrease in energy with mass number, reflecting the increase of quadrupole collectivity (cf. Fig. 1). ^{220,222}Th exhibit a quadrupole vibrational structure, whereas pronounced ground-state rotational bands with $E(4^+_1)/E(2^+_1) \approx 10/3$ are found in $^{226-232}$Th.

In Fig. 3(b) the calculated excitation energies of the negative-parity band form a parabolic structure centered between ^{224}Th and ^{226}Th. The approximate parabola of 1^-_1 states displays a minimum at ^{226}Th, in which the octupole deformed minimum is most pronounced (cf. Fig. 1), in agreement with the mass dependence of the experimental 1^-_1 level: $E(1^-_1) = 251$, 230, and 328 keV in ^{224,226,228}Th nuclei, respectively [37]. Starting from ^{226}Th, the energies of negative-parity states systematically increase and the band

becomes more compressed. A rotational-like collective band based on the octupole vibrational 1^-_1 state, that is, on the state that corresponds to nonstatic octupole deformation, develops. This result correlates with the systematics of microscopic energy surfaces that become softer in β_3 starting from ^{226}Th (Fig. 1), and with the increase (decrease) of the parameter ϵ_f ($|\chi_3|$) shown in Fig. 2(a) [2(b)]. The calculated negative-parity states for the lightest nuclei ^{220,222}Th are somewhat higher in energy when compared to the data [Fig. 3(b)]. The reason is that the valence space may not be large enough for these nuclei.

The vertex of the parabola of the calculated negative-parity states [Fig. 3(b)] can be associated with a QPT between stable octupole deformations and octupole vibrations characteristic for β_3-soft potentials, with the excitation energy of the negative-parity band (e.g., the 1^-_1 bandhead energy) representing the order parameter for this shape transition. Phenomenological studies (e.g., [12–15]) were only able to reproduce this QPT by employing Hamiltonians in which the degree of quadrupole-octupole correlations is controlled by a model parameter adjusted to the empirical position of the critical point. In contrast, the framework used in this Rapid Communication provides a fully microscopic prediction of the QPT. The shape phase transition occurs as a function of the physical control parameter—the nucleon (neutron) number, and the isotope ^{226}Th is found to be closest to the critical point. As we have already emphasized, in the case of atomic nuclei the control parameter of shape QPTs is discrete and, therefore, it is not always possible to associate a specific isotope to the critical point.

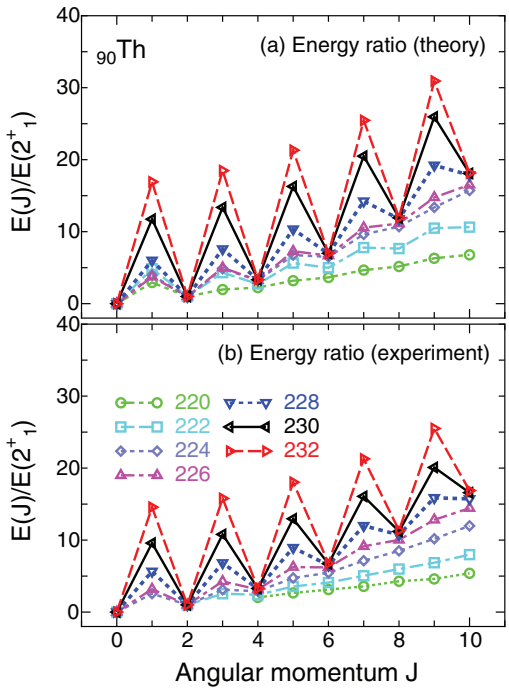

FIG. 4. (Color online) Theoretical (a) and experimental [37] (b) energy ratios $E(J)/E(2^+_1)$ of the yrast states of $^{220-232}$Th, including both positive (J even) and negative (J odd) parity, as functions of the angular momentum J.

Another indication of the phase transition between octupole deformation and octupole vibrations for β_3-soft potentials is provided by the odd-even staggering in the energy ratio $E(J)/E(2^+_1)$. Figure 4 displays the ratios $E(J)/E(2^+_1)$ for both positive- and negative-parity yrast states of $^{220-232}$Th as functions of the angular momentum J. Below ^{226}Th the odd-even staggering is negligible, indicating that positive and negative parity states are lying close to each other in energy. The staggering only becomes more pronounced starting from ^{228}Th, and this means that negative-parity states form a separate rotational band built on the octupole vibration. In particular, the energy ratio $E(J)/E(2^+_1)$ for negative-parity (odd-J) states could be considered as an order parameter for the octupole shape transition. We note that the predicted staggering of yrast states is in very good agreement with data [37].

To illustrate in more detail the level of quantitative agreement between our microscopic model calculation and data, in Fig. 5 we display the energy spectrum of positive and negative parity yrast states of the octupole-soft nucleus ^{230}Th, including the in-band $B(\mathrm{E2})$ values and the $B(\mathrm{E3}; 3^-_1 \to 0^+_1)$ (both in Weisskopf units), and the branching ratio $B(\mathrm{E1}; 1^-_1 \to 2^+_1)/B(\mathrm{E1}; 1^-_1 \to 0^+_1)$. The E1, E2, and E3 operators read $\hat{T}^{(E1)} = e_1(d^\dagger \times \tilde{f} + f^\dagger \times \tilde{d})^{(1)}$, $\hat{T}^{(E2)} = e_2\hat{Q}$ and $\hat{T}^{(E3)} = e_3(\hat{V}^\dagger_3 + \hat{V}_3)$, respectively, with the effective charges $e_2 = 0.19$ eb and $e_3 = 0.19$ eb$^{3/2}$ taken from previous empirical studies in Refs. [9] and [11], respectively. One notices a very good agreement with experiment [37,38], not only for excitation energies but also for transition probabilities.

Finally, we note that the connection between the evolution of collective excitations and the occurrence of a nuclear shape QPT has, in many studies, been investigated using symmetry-dictated approaches, including the IBM. In these studies the concept of a QPT is closely related to the group structure of a schematic IBM Hamiltonian, that is, a Hamiltonian of Ising type [20]. Since the number of shape degrees of

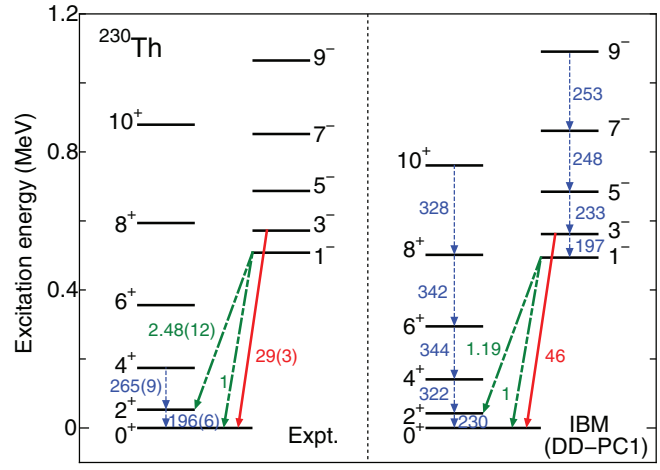

FIG. 5. (Color online) Experimental [37,38] and calculated yrast states of positive and negative parity in ^{230}Th. The in-band $B(\mathrm{E2})$ values (dotted) and the $B(\mathrm{E3}; 3^-_1 \to 0^+_1)$ (solid) (both in Weisskopf units), and the branching ratio $B(\mathrm{E1}; 1^-_1 \to 2^+_1)/B(\mathrm{E1}; 1^-_1 \to 0^+_1)$ (dashed-dotted) are also shown.

freedom becomes rather large when octupole deformation is taken into account, a major challenge is to develop a symmetry-dictated approach that captures the physics of both quadrupole and octupole collective degrees of freedom, thereby providing a phase diagram in the parameter space associated to a certain symmetry structure of the Hamiltonian. In the present work, on the other hand, the Hamiltonian in Eq. (1) takes the simplest possible form and the parameters are determined solely from the basic topology of the microscopic energy surface in the vicinity of its minimum and, therefore, no symmetry structure is imposed on the Hamiltonian. The development of a symmetry-dictated description of shape phase transitions considered in this Rapid Communication presents an interesting problem for future studies.

In summary, we have performed a microscopic analysis of a transition between stable octupole deformation and octupole vibrations in Th isotopes. A global relativistic EDF, not specifically adjusted to octupole degrees of freedom nor applied to reflection-asymmetric nuclei, has been used to calculate axially symmetric constrained energy surfaces in the (β_2,β_3) plane. The sdf-IBM Hamiltonian has been constructed by mapping the microscopic energy surface onto the equivalent one in the boson system, providing the low-energy excitation spectra and transition rates, that is, observables that can be related to quantum order parameters. The microscopic model predicts a transition from spherical shapes near ^{220}Th to stable octupole and quadrupole deformations around ^{226}Th, and the development of octupole vibrations characteristic for β_3-soft potentials in heavier Th nuclei. The EDF constrained microscopic energy surfaces (Fig. 1) and the systematics of low-energy excitation spectra (Figs. 3 and 4) point to the occurrence of a shape phase transition near ^{226}Th. With increasing neutron number the octupole deformation appears to be β_3 unstable (soft) and remains such up to ^{232}Th. This result is in excellent agreement with available data and previous phenomenological studies of phase transitions in octupole collective degrees of freedom. Based on a comparison with previous work, it appears that Th presents the best case for octupole deformations in atomic nuclei.

The authors would like to thank R. V. Jolos and J. Zhao for useful discussions. K.N. acknowledges support by the JSPS postdoctoral programs for research abroad. Calculations were partly performed on the ScGrid of the Supercomputing Center, Computer Network Information Center of Chinese Academy of Sciences.

[1] A. Bohr and B. M. Mottelsson, *Nuclear Structure*, Vol. 2 (Benjamin, New York, 1975).
[2] P. Ring and P. Schuck, *The Nuclear Many-Body Problem* (Springer-Verlag, Berlin, 1980).
[3] R. F. Casten, *Nuclear Structure from a Simple Perspective* (Oxford University Press, Oxford, 1990).
[4] P. A. Butler and W. Nazarewicz, Rev. Mod. Phys. **68**, 349 (1996).
[5] O. Scholten, F. Iachello, and A. Arima, Ann. Phys. (NY) **115**, 325 (1978).
[6] W. Nazarewicz, P. Olanders, I. Ragnarsson, J. Dudek, G. A. Leander, P. Möller, and E. Ruchowsa, Nucl. Phys. A **429**, 269 (1984).
[7] P. Bonche, P.-H. Heenen, H. Flocard, and D. Vautherin, Phys. Lett. B **175**, 387 (1986).
[8] J. Engel and F. Iachello, Nucl. Phys. A **472**, 61 (1987).
[9] T. Otsuka and M. Sugita, Phys. Lett. B **209**, 140 (1988).
[10] D. Kusnezov and F. Iachello, Phys. Lett. B **209**, 420 (1988).
[11] P. D. Cottle and N. V. Zamfir, Phys. Rev. C **58**, 1500 (1998).
[12] P. G. Bizzeti and A. M. Bizzeti-Sona, Phys. Rev. C **70**, 064319 (2004).
[13] D. Bonatsos, D. Lenis, N. Minkov, D. Petrellis, and P. Yotov, Phys. Rev. C **71**, 064309 (2005).
[14] D. Lenis and D. Bonatsos, Phys. Lett. B **633**, 474 (2006).
[15] P. G. Bizzeti and A. M. Bizzeti-Sona, Phys. Rev. C **77**, 024320 (2008).
[16] P. G. Bizzeti and A. M. Bizzeti-Sona, Phys. Rev. C **81**, 034320 (2010).
[17] R. V. Jolos, P. von Brentano, and J. Jolie, Phys. Rev. C **86**, 024319 (2012).
[18] R. Rodríguez-Guzmán, L. M. Robledo, and P. Sarriguren, Phys. Rev. C **86**, 034336 (2012).
[19] N. Minkov, S. Drenska, M. Strecker, W. Scheid, and H. Lenske, Phys. Rev. C **85**, 034306 (2012).
[20] P. Cejnar, J. Jolie, and R. F. Casten, Rev. Mod. Phys. **82**, 2155 (2010).
[21] F. Iachello and A. Arima, *The Interacting Boson Model* (Cambridge University Press, Cambridge, 1987).
[22] M. Bender, P.-H. Heenen, and P.-G. Reinhard, Rev. Mod. Phys. **75**, 121 (2003).
[23] T. Nikšić, D. Vretenar, and P. Ring, Phys. Rev. C **78**, 034318 (2008).
[24] T. Nikšić, D. Vretenar, and P. Ring, Prog. Part. Nucl. Phys. **66**, 519 (2011).
[25] Z. P. Li, J. M. Yao, D. Vretenar, T. Nikšić, H. Chen, and J. Meng, Phys. Rev. C **84**, 054304 (2011).
[26] V. Prassa, T. Nikšić, G. A. Lalazissis, and D. Vretenar, Phys. Rev. C **86**, 024317 (2012).
[27] D. Vretenar, A. V. Afanasjev, G. Lalazissis, and P. Ring, Phys. Rep. **409**, 101 (2005).
[28] B.-N. Lu, J. Zhao, E.-G. Zhao, and S.-G. Zhou, arXiv:1304.2513; B.-N. Lu, E.-G. Zhao, and S.-G. Zhou, Phys. Rev. C **85**, 011301(R) (2012).
[29] Y. Tian, Z. Y. Ma, and P. Ring, Phys. Lett. B **676**, 44 (2009).
[30] T. Otsuka, A. Arima, and F. Iachello, Nucl. Phys. A **309**, 1 (1978).
[31] A. F. Barfield, B. R. Barrett, J. L. Wood, and O. Scholten, Ann. Phys. (NY) **182**, 344 (1988).
[32] K. Nomura, N. Shimizu, and T. Otsuka, Phys. Rev. Lett. **101**, 142501 (2008).
[33] J. N. Ginocchio and M. W. Kirson, Nucl. Phys. A **350**, 31 (1980).
[34] K. Nomura, N. Shimizu, and T. Otsuka, Phys. Rev. C **81**, 044307 (2010).
[35] D. Kusnezov, computer program OCTUPOLE (unpublished).
[36] K. Nomura, T. Otsuka, N. Shimizu, and L. Guo, Phys. Rev. C **83**, 041302 (2011).
[37] Brookhaven National Nuclear Data Center, http://www.nndc.bnl.gov.
[38] B. Ackermann, H. Baltzer, C. Ensel, K. Freitag, V. Grafen, C. Günther, P. Herzog, J. Manns, M. Marten-Tölle, U. Müller *et al.*, Nucl. Phys. A **559**, 61 (1993).